THE EARTHQUAKE RESPONSE OF PRESTRESSED CONCRETE STRUCTURES WITH NONSTRUCTURAL INTERFLOOR ELEMENTS

by Richard A. Spencer[I]

SYNOPSIS

The effect of nonstructural interfloor elements on the nonlinear earthquake response of a twenty story prestressed concrete frame structure is discussed. The idealized elements can have either yielding or essentially linear hysteretic behaviour, and can be included at any story level. Twelve comparative studies suggest that the elements can control interstory drift effectively, and have little effect on total story shear forces.

INTRODUCTION

Many studies have been made — e.g.: (1), (2), (3), (4) — of the nonlinear response of tall structures subjected to earthquake excitation. In these studies the columns and girders are generally assumed to be able to yield, so that they dissipate considerable energy during the earthquake. In addition, viscous damping is often included to take account of the additional energy dissipation assumed to occur in other structural and nonstructural elements.

However, there is evidence that most damping in structures is essentially frequency independent, (5), (6), (7), and therefore, is not correctly represented by viscous damping. In this study nonlinear response parameters are discussed for a prestressed concrete structure with nonstructural interstory elements, which stiffen the structure and have force-deflection properties which are independent of frequency.

STRUCTURE ANALYZED

The twenty story structure analyzed (see figure 1) was originally designed by Clough, Benuska and Lin (2). Member flexural rigidities were specified in terms of a reference value, EI_o = 133,500 Kip. ft^2 (see Table 1), which gave a natural period of 2.2 seconds. An analysis was then made to find the "design" moments resulting from static application of code (8) horizontal and vertical design forces. For the prestressed concrete version studied here, cracking moments were taken as twice the design moments for the girders, and six times the design moments for the columns. The same structure has been studied before by the author (4).

[I]Assistant Professor, Department of Civil Engineering, University of British Columbia, Vancouver, Canada.

PRESTRESSED FRAME MEMBERS

The form of the idealized end moment-end rotation (M_e - θ_e) hysteresis loops used for the prestressed concrete columns and girders is shown in figure 2. They are based on experimental results (6) for the load case of equal end moments producing reversed curvature. Each loop is defined by the stiffness, S_1, of the member with all cracks closed by prestress, and four other parameters defined as shown in figure 2: the cracking moment, M_c; the stiffness reduction factor, p; the reversal stiffness factor, p_r; and the loopwidth factor, ℓ. Values used here were: for the columns, p = 0.5 and ℓ = 0.05; and for the girders, p = 0.2 and ℓ = 0.2. These values reflect the higher ratio of cracking to design moment for the columns. It is assumed that reversal can occur at any value of θ_e, with p_r = 2.0 in all cases.

The model member used to represent each prestressed frame member is described in detail elsewhere (9).

VISCOUS DAMPING

To find some energy dissipation values it was necessary to let the structure come to rest after the earthquake excitation ended. A small amount of mass proportional viscous damping was included to bring the structure to rest in a reasonable time. Taking the fraction of critical damping, ξ_m, as 0.005, ensured that the viscous force acting on any floor never exceeded 1 Kip, which was small in comparison with other forces acting.

NONSTRUCTURAL ELEMENTS

Nonstructural interstory connecting elements were used to try and model the effect of partitions, walls etc., on the response of real structures. Because there is little experimental evidence available on the behaviour of such elements under earthquake loading, idealized elements were used here. Each element was assumed to be able to resist relative interstory displacements (drift) by exerting equal and opposite horizontal forces on adjacent floors.

A Ramberg-Osgood function, with an appropriate hysteresis law, was used to define the force-deformation hysteresis loops on which the element loops were based. The equation of the skeleton curve (figure 3) can be written:

$$\frac{x}{x_y} = \frac{f}{f_y} + \alpha\left(\frac{f}{f_y}\right)^r$$

where x is the interstory drift, f is the force exerted on the floors, x_y and f_y define "yield values", α is a positive number, and r is a positive, odd, integer.

The equation of the two branch curves originating at $P_1(x_1, f_1)$ and $-P_1(-x_1, -f_1)$ on the skeleton curve, and forming a closed hysteresis loop

(see figure 3) is:

$$\frac{x \mp x_1}{2x_y} = \frac{f \mp f_1}{2f_y} + \alpha\left(\frac{f \mp f_1}{2f_y}\right)^r$$

The hysteresis law is illustrated in figure 4. Loading always begins along the skeleton curve, and the first reversal at P_1 defines a minimum and a maximum curve. These are branch curves originating at P_1 and $-P_1$ respectively. The maximum and minimum curves become tangent to the skeleton curve at P_1 and $-P_1$ respectively.

If the second reversal, at P_2, occurs before the point $-P_1$ is reached, the maximum and minimum curves become boundaries for the force-deformation behaviour. If a branch curve subsequently intersects the maximum or minimum curve, further loading is along that curve until the next reversal occurs, or loading proceeds beyond P_1 or $-P_1$. In the latter case loading then proceeds along the skeleton curve, until the next reversal (at P_3) defines new minimum and maximum curves originating at P_3 and $-P_3$. These become the new boundaries for the force-deformation behaviour until loading proceeds beyond P_3 or $-P_3$.

It should be noted that an ascending branch, originating anywhere inside the loop formed by maximum and minimum curves, will (if there is no reversal) always intersect the maximum curve, and never the minimum curve.

In this analysis the elements were assumed to be linear during successive small time increments, and their force-deflection properties were represented by continuous, piece-wise linear loops, which had the same gradient as the curvilinear loops at the start of every time interval. The forces vary somewhat from those defined by the curvilinear loops and the hysteresis law, but the variation is small when the time increment is small. The Newton-Raphson iterative technique was used to solve the Ramberg-Osgood equation after each time interval.

Two basic loops were used to describe the nonstructural elements (see figures 5(a) and 5(b)). The loops with $r = 11$ and $\alpha = 0.2$ represented yielding behaviour with considerable energy dissipation. Those with $r = 3$ and $\alpha = 0.01$ represent more nearly linear force-deformation behaviour.

Values of f_y were taken as 30 or 60 Kips (except in one case). Since the structure has a three bay frame, elements with "yield strengths" of 10 or 20 Kips in each bay would give the assumed values of f_y. These yield strengths should be attainable with real elements. Values of x_y were taken as 0.1 or 0.5 inches to represent "hard" and "soft" elements.

It must be noted that there is no provision for the loss of stiffness and strength which most yielding elements would suffer if x/x_y greatly exceeded one. Thus in some cases studied here, the idealization is probably rather unrealistic. However, the yielding behaviour assumed could result from elastic element deformation, followed by slip rather than yielding, which would not necessarily result in damage.

NONLINEAR EQUATIONS OF MOTION

The nonlinear equations of motion were solved using a step-by-step integration technique, with the structure assumed to remain linear during each of a series of time increments. Deformations were checked at the end of each time increment, and the stiffness matrix was changed if necessary to reflect the nonlinear behaviour of the members and elements. The time increment was 0.005 seconds.

The foundation of the structure was assumed to be rigid and torsion was neglected. Masses were concentrated at the floors, which moved only horizontally and contributed no stiffness.

EXCITATION

The excitation used was the first 8 seconds of the N-S component of the 1940 El. Centro earthquake. This record has a peak acceleration of 0.32g, which occurs 2 seconds after the start of the record.

RESULTS PRESENTED

This study is concerned with the effect of nonstructural interfloor elements on response. The response parameters of greatest interest are the maximum values of: the interstory drift; the story shear force in the columns, V_c, and in the nonstructural elements, V_n; and the total story shear, V_t, where:

$$V_t = V_c + V_n$$

Even although the two maxima which are summed to get V_t may not occur simultaneously on any given floor, values of V_t do suggest adequate total story shear capacities for an El. Centro type earthquake. Figure 14 shows some values of V_t, and the envelope inside which all the values lie.

Cumulative totals for energy dissipated by the columns and girders, D_s, the nonstructural elements, D_n the viscous dampers, D_v, and the total structure, D_t, are also discussed. The presence of nonlinear elements — structural and nonstructural — makes it impossible to predict how much of the energy stored in the nonstructural elements can be regarded as dissipated when the excitation ends, (and energy input ceases), and how much can be regarded as recoverable strain energy. In this study D_n was found by continuing the step-by-step integration until every story underwent a displacement of less than 0.0005 in. during a time interval.

In a real structure, energy dissipation is usually associated with localized damage to the elements involved. On the other hand, dissipation of energy might be expected to reduce the amplitude of the vibrations that build up during an earthquake, and so reduce damage due to large deformations. The prestressed structural elements assumed here, which do not yield when their stiffness falls due to cracking, can dissipate energy without being damaged. However, as already

mentioned, it is probable that real nonstructural elements would suffer serious damage if called upon to dissipate significant amounts of energy by yielding.

The total energy input to the structure, E_i, was also computed. It will be seen that high values of E_i are associated with large maximum displacements — both interstory and absolute — regardless of whether or not there is a large total energy dissipation, D_t.

Maximum values of the nonlinear deformations in the nonstructural elements, $(x/x_y)_{max}$, are tabulated to indicate likely damage, and whether or not the element modelled is realistic. Nonlinear member deformations are measured by maximum values of the ductility factor, μ, defined as:

$$\mu = \frac{\theta_{max}}{\theta_1} \quad \begin{matrix} (\text{if } \theta_{max} < \theta_c,\ \theta_1 = \theta_c) \\ (\quad \theta_{max} > \theta_c,\ \theta_1 = \theta_\ell) \end{matrix}$$

where θ_ℓ is defined in figure 2.

Maximum values of base overturning moment, M_b, and the compressive force at the base of the exterior column, F_c, result from dynamically induced moments and shears, not gravity or dead load effects. Values of maximum displacement at the 20th story, U_{20}, and the maximum story acceleration, A, are also tabulated.

Because of the simplifying assumptions and idealizations that are necessary, an analysis of this type may not give accurate quantitative predictions of structural response. However, by comparing results for different structures, it is possible to understand the qualitative effect of various structural changes on response.

DISCUSSION OF RESULTS

The structure was analyzed eleven times with varying combinations of nonstructural elements, (and once with none). One of these structures had reduced column cracking moments. Structural properties are summarized in Table 2.

Structure 1 had nonstructural elements at every story, defined by f_y = 30 Kips, x_y = 0.1 in., r = 11 and α = 0.2, (see Table 2). Thus these elements were relatively stiff, with a well defined, relatively low yield point. This structure had mass proportional viscous damping with ξ_m= 0.005, and its response is compared first with that of structure 2, which was identical except that there was no viscous damping. The relatively small effect of this damping can be seen from figures 6 and 10, and from Tables 3 and 4. All structures except structure 2 had ξ_m = 0.005. Viscous energy dissipations are shown in Table 3.

The interstory drifts for structure 1 (figure 6), when compared with those obtained for a version of the structure with elasto-plastic members, ξ_m = 0.10 and no nonstructural elements (4), are generally somewhat larger, and have a

different distribution with respect to height. However, the largest drift for structure 1 is only 0.06 inches greater than that for the elasto-plastic structure, so on this basis their performances appear to be equally satisfactory.

Structure 3 had no nonstructural elements. Interstory drifts (figure 6) were much higher than for structure 1, and higher than those of any other structure. The story shears in the columns, V_c (figure 10) were also the highest recorded, but they were no greater than the total story shears, V_t, for some of the other structures. Values of D_s, D_v and E_i (Table 3), and M_b, F_c, and U_{20} (Table 4), were also the highest recorded.

Structure 4 was similar to structure 1, except that all the nonstructural elements were softer, having $x_y = 0.5$ in. instead of 0.1 in. This resulted in interstory drifts that were greater at every floor than those for structure 1 (figure 6), although they were less than those for structure 3. Story shears in the columns were greater than those for structure 1, (figure 10) and total story shears were comparable with the column story shears for structure 3.

In spite of the higher interstory drifts, the use of $x_y = 0.5$ for structure 4 gives $(x/x_y)_{max} = 3.16$ (compared to 13.6 for structure 1), (Table 4). It is possible that real elements might be able to withstand several cycles of loading of this severity without undue loss of strength.

The overturning moment at the base, $M_b = 91 \times 10^3$ Kip. ft., and the dynamically induced compression in the exterior base column, $F_c = 1412$ Kips., were both relatively high. The dead load contribution to M_b found by simultaneously giving each story its maximum lateral displacement was less than 60×10^3 Kip. ft., so that from this point of view lateral displacements of about 20 inches at top of the structure are not excessive. Since the static moment required to overturn the structure (dead load only) is 154×10^3 Kip. ft., M_b is probably not dangerously high, and it is F_c which is more significant.

The compression in the exterior base column due to the static application of dead plus live loads is 1100 Kips., and the application of Code (10) lateral forces, (with no reduction factor for overturning moment) adds only another 340 Kips. Thus this analysis suggests that exterior columns for this structure could be seriously underdesigned by static design methods. Note that even for structure 1, $F_c = 1254$ Kips.

The maximum story acceleration was A = 1.27g, (recorded at the 14th floor), whereas the Code (10) assumes that 1g is a reasonable maximum. For structure 1, A was only 0.614g.

There appear to be severe consequences for the structure when the stiffness of the nonstructural elements is reduced.

In structure 5 the nonstructural elements had hysteresis loops described by $r = 3$, $\alpha = 0.02$ (see figure 5(b)). Their stiffness was the same as those in structure 1, i.e.: $f_y = 30$ kips. and $x_y = 0.1$ in. The interstory drifts for this structure (figure 7) are generally much less than those of structure 1, and have a maximum of only .78 in. However, this implies that $(x/x_y)_{max} = 7.8$,

and the story shears in the nonstructural elements are correspondingly high (figure 11). The energy input is higher than for structure 1, and the energy dissipation is less, (Table 3), but the more nearly linear nonstructural elements are more effective in controlling deflection than the yielding elements of structure 1.

It is worth noting that diagonal bracing wires with the required stiffness and adequate strength, could be designed to replace the nonstructural elements assumed in structure 4. However, diagonal bracing of this type could contribute axial compressive forces to the exterior columns on one side of the structure, which could sum to a value comparable to F_c under some conditions. Thus careful checking of the exterior column capacities would be required before such bracing was used. There are also likely to be architectural reasons for not incorporating bracing of this type.

Structure 6 was similar to structure 5, except that x_y was increased from 0.1 to 0.5, making the nonstructural elements less stiff, but still linear rather than yielding. Whereas interstory drifts for structure 5 were generally less than those for structure 1, those for structure 6 were all greater (figure 7). Story shears in the columns, V_c, were also greater than for structure 5 (figure 11), and total story shears were the highest of any structure at some stories (figure 14). The maximum story acceleration of 1.31g on the 15th floor was also the highest value found.

Because $(x/x_y)_{max}$ was equal to 3.36, the hysteresis loop was always small, and the nonstructural energy dissipation, D_n = 24 Kip. ft., was the lowest recorded. The combination of low stiffness and small energy dissipation results in nonstructural elements which are relatively ineffective in controlling response.

Structure 7 had columns with cracking moments reduced from six times to twice the design moments, and $M_e - \theta_e$ loops the same as those for the girders ($p = 0.2$, $\ell = 0.2$). This represents a more practical prestressed design, and the nonlinear deformations were generally greater in the columns than in the girders. (In the other structures cracking in the columns was generally restricted to the first story, and the results would have been little different if the columns had been plain reinforced concrete.)

The nonstructural elements were the same as for structure 1, and interstory drift was very similar for both structures (figure 7). The story shears in the columns of structure 7 were all slightly lower than those of structure 1, (figure 11) and the total story shears for the 8th to the 20th story were the lowest found. In general, reducing the column cracking moments is seen to have little effect on the response, which is generally similar to that of structure 1, and is thus satisfactory when compared to the elasto-plastic structure mentioned previously (4). Note, however, that $(x/x_y)_{max}$ was nearly 15 for both structure 1 and structure 7, so that there must be some reservations about the modelling of the nonstructural elements.

Structures 8, 9 and 10 had no nonstructural elements stiffening the first 5 stories. The remaining 15 stories of structure 8 had the same elements as structure 1 (see Table 2). The interstory drifts (figure 8) were somewhat greater than for structure 1 over most of the height of the structure, and

were not noticeably exaggerated for the lower stories. The story shears (figure 12) were much the same as those for structure 1.

In structure 9, f_y was increased from 30 to 60 Kips. Since x_y remained 0.1 inches, the stiffness was effectively doubled. These elements were effective in reducing interstory drift above the 5th story, and although interstory drift was higher in the first five stories, the maximum value was still less than that for structure 1 (figure 8). Story shears in the columns, were predictably lower, and those in nonstructural elements higher, than in structure 1 (figure 12). However, their sum, V_t, was not very different from that for structure 1.

Structure 10 had f_y increased to 300 Kips., with $x_y = 0.1$. Thus these elements were ten times as strong and ten times as stiff as those in structures 1 and 8. In fact these elements would transform the structure into a bending structure, for which the nonlinear analysis is no longer strictly valid. The results are still of some interest, however. Firstly, they show interstory drifts in the first five stories which are not particularly high compared to those of the other structures. And secondly, the sum of the story shears, V_t, was similar to that of the other structures.

The conclusion for structures 8, 9 and 10 seems to be that lower stories which are more flexible than the rest of the structure do not lead to excessive shears and deflections in those stories.

Structure 11 was similar to structure 1, except that the nonstructural elements were removed for stories 9, 10, 11 and 12. The interstory drift was similar to that of structure 1 at the top and bottom of the structure, and larger from the 6th to the 14th story (figure 9). Other response parameters were generally a little larger than those of structure 1, but the increases suggest no serious consequences as a result of the more flexible middle section of the structure.

Structure 12 had nonstructural elements similar to those of structure 1 (f_y = 30 Kips., $x_y = 0.1$, $r = 11$ and $\alpha = 0.2$), but incorporated at the 5th, 8th, 11th, 14th and 17th stories only. These elements were ineffective in reducing the interstory drift, which at some stories was nearly as large as for structure 3, which had no nonstructural elements at all. Other response parameters (Table 3) were all relatively high.

CONCLUSIONS

The following conclusions, which apply only to the structures studied, can be drawn:

1. The nonstructural interstory elements can be very effective in reducing interstory drift.

2. Nonyielding elements with low energy dissipation tend to be more effective than yielding elements which dissipate more energy.

3. Varying the nonstructural elements has little effect on the total story shears.

4. Omitting the elements in a few stories has no severe consequences.

5. Compressive forces in the lower story exterior columns, and maximum story accelerations, appear to be higher than assumed in practice.

ACKNOWLEDGEMENTS

This study was supported by a grant from the National Research Council.

BIBLIOGRAPHY

1. Clough, R.W. and Benuska, K.L., "Nonlinear Earthquake Behavior of Tall Buildings," Proc. ASCE, Vol.93, No.EM3, June 1967.

2. Clough, R.W., Benuska, K.L. and Lin, T.Y., "FHA Study of Seismic Design Criteria for High Rise Buildings," Report HUD TS-3, Federal Housing Administration, Washington, D.C., August 1966.

3. Giberson, M.F., "The Response of Nonlinear Multi-Story Structures Subjected to Earthquake Excitation," Ph.D. thesis, California Institute of Technology, May 1967.

4. Spencer, R.A., "The Nonlinear Response of a Multistory Prestressed Concrete Structure to Earthquake Excitation," Proc. 4th World Conference on Earthquake Engineering, Chile, 1969.

5. Medearis, K. and Young, D.H., "Energy Absorption of Structures Under Cyclic Loading," Proc. ASCE, V.90, No.ST1, February 1964.

6. Spencer, R.A., "Stiffness and Damping of Nine Cyclically Loaded Prestressed Concrete Members," Journal of the Prestressed Concrete Institute, Vol.14, No.3, June 1969.

7. Bertero, V.V., "Seismic Behavior of Steel Beam-to-Column Connection Subassemblages," Proc. 4th World Conference on Earthquake Engineering, Chile, 1969.

8. "Uniform Building Code," Int. Conf. of Building Officials, Calif., 1964.

9. Spencer, R.A., "The Nonlinear Response of Some Multistory Reinforced and Prestressed Concrete Structures Subjected to Earthquake Excitation." California Institute of Technology, Novemeber 1968.

10. "National Building Code of Canada 1970," National Research Council, Ottawa.

TABLE 1: RELATIVE FLEXURAL RIGIDITIES OF STRUCTURAL MEMBERS

Story Levels	EI/EI_o		
	Columns		Girders
	Exterior	Interior	
20-18	1.0	2.0	4.0
17-15	1.5	3.0	6.0
14-12	3.0	6.0	8.0
11-9	4.5	9.0	
8-6	6.0	12.0	
5-3	10.0	20.0	10.0
2-1	12.0	24.0	

TABLE 2: DETAILS OF NONSTRUCTURAL ELEMENTS FOR EACH STRUCTURE

Structure No.	Yield Force fy(Kips)	Yield Disp. xy(inches)	Ramberg-Osgood Parameters		Location of Elements
			r	α	
1	30.0	0.1	11	0.2	All Stories
2	30.0	0.1	11	0.2	All Stories
3					None
4	30.0	0.5	11	0.2	All Stories
5	30.0	0.1	3	0.01	All Stories
6	30.0	0.5	3	0.01	All Stories
7	30.0	0.1	11	0.2	All Stories
8	30.0	0.1	11	0.2	Stories 6-20
9	60.0	0.1	11	0.2	Stories 6-20
10	300.0	0.1	11	0.2	Stories 6-20
11	30.0	0.1	11	0.2	Stories 1-8 and 13-20
12	30.0	0.1	11	0.2	Stories 5, 8, 11, 14 and 17

TABLE 3: ENERGY VALUES (CUMULATIVE TOTALS)

Structure No.	ENERGY DISSIPATED (Kip. ft)				Energy Input (Kip. ft) E_i
	Cols. and Girders D_s	Nonstruc. Elements D_n	Viscous Dampers D_v	Total D_t	
1	274	339	37	650	1080
2	284	352	—	636	1090
3	720	—	127	847	2050
4	457	167	71	695	1455
5	309	118	34	461	1200
6	592	24	95	711	1805
7	295	350	41	686	1140
8	339	297	52	688	1260
9	248	327	34	609	1040
10	222	108	25	355	1215
11	334	307	48	689	1220
12	516	174	83	773	1630

TABLE 4: MAXIMUM VALUES OF VARIOUS RESPONSE PARAMETERS

Structure No.	Element Def. $(x/x_y)_{max}$	Ductility Factor μ		O'turning Moment ($Kip.ft \times 10^3$) M_b	Ext. Col Force (Kips) F_c	Top Story Disp. (in) U_{20}	Story Accel. (g) A
		Column	Girder				
1	13.6 (6)*	1.87 (1)*	2.63 (6)*	82	1254	14.87	0.61 (6)*
2	14.09 (6)	1.89 (1)	2.64 (4)	84	1282	15.52	0.62 (20)
3	—	1.95 (1)	3.50 (18)	100	1571	26.49	1.22 (14)
4	3.16 (9)	1.95 (1)	2.93 (8)	91	1412	19.92	1.27 (14)
5	7.8 (2)	0.91 (1)	2.1 (1)	63	933	9.16	0.88 (20)
6	3.36 (9)	1.88 (1)	3.11 (9)	92	1414	20.64	1.31 (15)
7	14.84 (6)	3.91 (1)	2.54 (4)	77	1210	16.85	0.83 (7)
8	15.53 (6)	2.02 (1)	2.88 (4)	91	1388	18.07	0.69 (14)
9	11.64 (6)	2.01 (1)	2.85 (4)	78	1173	12.79	0.54 (5)
10	3.19 (6)	1.86 (1)	2.46 (3)	47	579	5.43	0.56 (20)
11	14.6 (7)	1.87 (1)	2.79 (8)	87	1341	17.37	0.78 (14)
12	15.6 (11)	1.98 (1)	2.98 (9)	95	1489	23.01	1.05 (14)

*Story where this value occurred

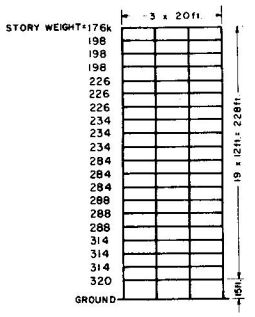

Figure 1: PROPERTIES OF STRUCTURE.

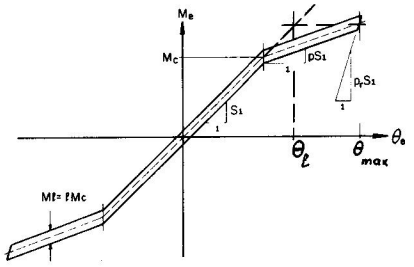

Figure 2: TYPICAL $M_e - \theta_e$ LOOP FOR A psc MEMBER.

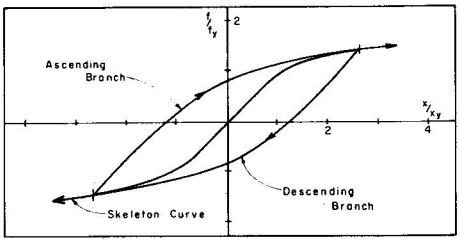

Figure 3: TYPICAL RAMBERG-OSGOOD SKELETON AND BRANCH CURVES.

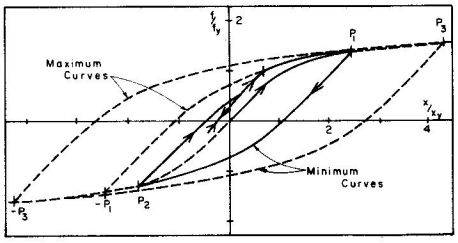

Figure 4: ILLUSTRATION OF RAMBERG - OSGOOD HYSTERESIS LAW.

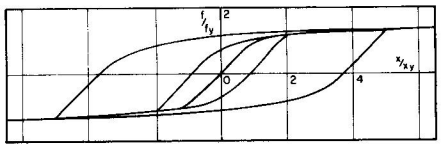

Figure 5(a): SKELETON CURVE AND TYPICAL HYSTERESIS LOOPS, r = 11, α = 0.2

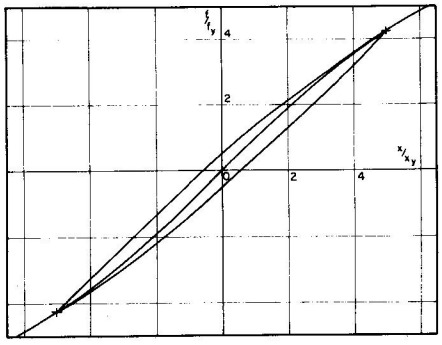

Figure 5(b): SKELETON CURVE AND TYPICAL HYSTERESIS LOOPS, r = 3, α = 0.01

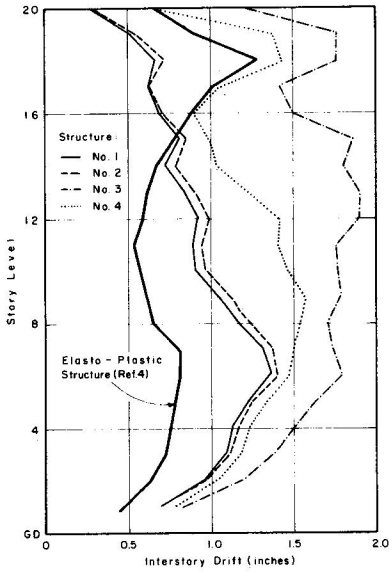

Figure 6: INTERSTORY DRIFT FOR STRUCTURES 1,2,3,4 AND ELASTO-PLASTIC STRUCTURE (Reference 4).

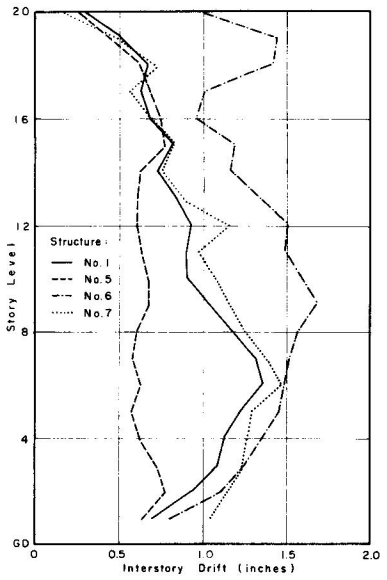

Figure 7: INTERSTORY DRIFT FOR STRUCTURES 1,5,6 & 7.

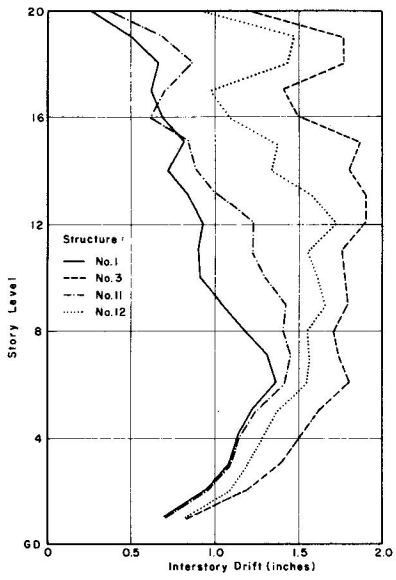

Figure 9: INTESTORY DRIFT FOR STRUCTURES 1,3, 11 & 12.

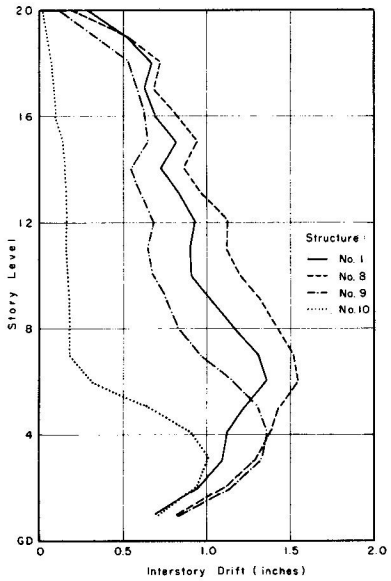

Figure 8: INTERSTORY DRIFT FOR STRUCTURES 1,8,9 & 10.

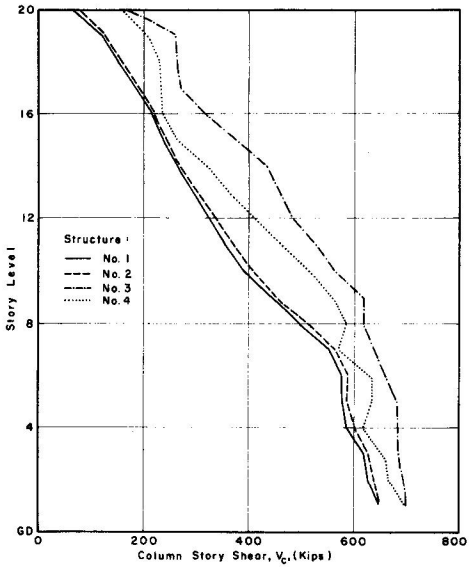

Figure 10: COLUMN STORY SHEAR, V_c, FOR STRUCTURES 1, 2, 3 & 4.

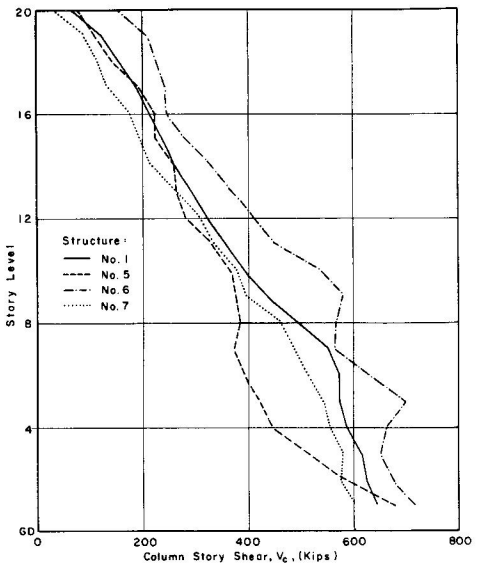

Figure 11 : COLUMN STORY SHEARS, V_c, FOR STRUCTURES 1, 5, 6 & 7.

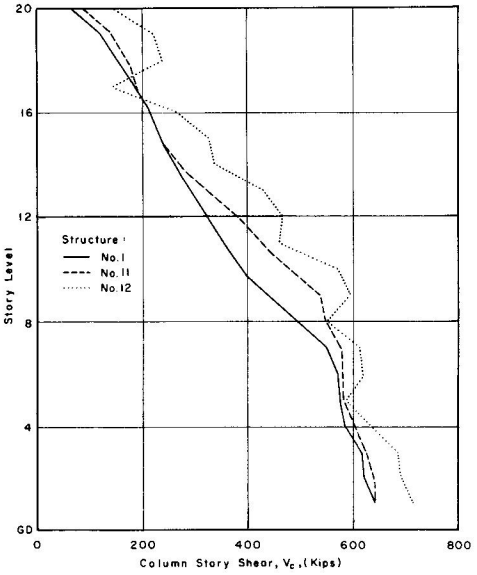

Figure 13 : COLUMN STORY SHEARS, V_c, FOR STRUCTURES 1, 11 & 12.

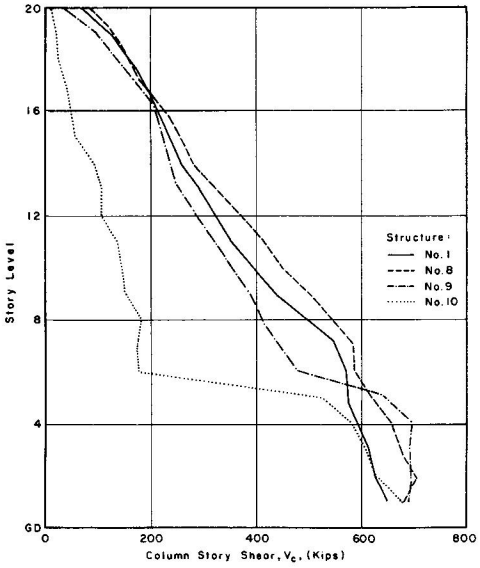

Figure 12 : COLUMN STORY SHEAR, V_c, FOR STRUCTURES 1, 8, 9 & 10.

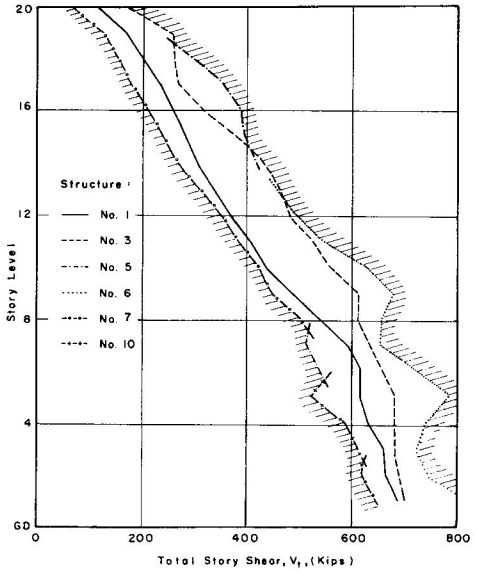

Figure 14 : ENVELOPE FOR TOTAL STORY SHEAR, V_t.